Christian Funk, Jürgen Köhler and Thomas Schleid*

A series of new layered lithium europium(II) oxoniobates(V) and -tantalates(V)

https://doi.org/10.1515/znb-2019-0190
Received November 8, 2019; accepted November 18, 2019

Abstract: The new Ruddlesden-Popper-related phases $A_{n+1}B_nO_{3n+1}$ ($n=3$) with the compositions $Li_2Eu_2Nb_3O_{10}$, $Li_2Eu_{1.5}Ta_3O_{10}$, $Li_2EuKNb_3O_{10}$, and $Li_2EuKTa_3O_{10}$ were synthesized by solid-state reactions from $Li_2[CO_3]$ (+ $K_2[CO_3]$) and the corresponding refractory metals along with their oxides in a high-frequency furnace at temperatures above $T=1600$°C. Their structures have been determined by single-crystal X-ray diffraction studies. Characteristic features are triple layers of corner-sharing $[MO_6]^{7-}$ octahedra (M = Nb and Ta), which are connected via $[LiO_4]^{7-}$ tetrahedra. The Eu^{2+} cations are cuboctahedrally surrounded by 12 oxygen atoms and according to the Eu–O distances of around 275 pm, they have the oxidation state +2, as confirmed by XPS measurements. In the potassium-containing samples they share their positions with K^+ cations. The black compounds are stable in air at room temperature. Measurements of the magnetic susceptibilities in the range of $T=5$–300 K revealed $Li_2Eu_2Nb_3O_{10}$, $Li_2Eu_{1.5}Ta_3O_{10}$ and $Li_2EuKTa_3O_{10}$ to be paramagnetic without any ordering.

Keywords: crystal structure analysis; europium; magnetism; oxoniobates; oxotantalates; Ruddlesden-Popper phases; XPS studies.

Dedicated to: Professor Arndt Simon on the occasion of his 80th birthday.

1 Introduction

Perovskite-type oxides with the overall formula ABO_3 have been studied for decades because of their interesting physical properties, and $BaTiO_3$ with its very high dielectric constant is only one prominent example [1]. For tuning the physical properties of such compounds numerous studies were carried out with magnetic cations on the B site. Investigations of perovskite-type compounds with highly paramagnetic Eu^{2+} cations on the A site have attracted particular attention. McCarthy and Greedan have proposed a few rules in 1974, which allow to predict the composition and properties of europium oxometalates ($EuMO_3$) [2], and meanwhile a whole series of such oxides has been described, e.g. $EuMO_3$ (M = Ti, Zr, Hf, Nb, etc.) [3–7]. Phase-pure $EuTiO_3$ was first synthesized in 1953 [8]. It becomes antiferromagnetic below $T=5.7$ K. The respective phase transition is accompanied by a drop in the dielectric constant, owing to a strong spin-lattice coupling [9], and therefore a magnetostriction effect is observed at low temperatures [10]. In addition, the development of 2D magneto-optical devices based on $EuTiO_3$ [11] appears possible. A common occupation of the A site by Sr^{2+} and Eu^{2+} leads to an interesting diluted magnetic system in the series $Eu_xSr_{1-x}TiO_3$ [12]. More complex oxides like the double perovskites ($A'AB_2O_6$, e.g. Eu_2ScTaO_6 with elpasolite-type structure) [13], the layered perovskite analogues, such as Dion-Jacobson ($RbLaNb_2O_7$), Aurivillius ($(Bi_2O_2)Bi_2Ti_3O_{10}$) [14] and Ruddlesden-Popper phases with the general formula $A_{n+1}M_nO_{3n+1}$, where n corresponds to the number of $^2_\infty\{[MO^{v}_{4/2}O^{t}_{2/1}]^{n-}\}$ layers of vertex-connected $[MO_6]^{7-}$ octahedra, have also been studied [15]. With $n=1$, monolayers of corner-sharing $[MO_6]^{n-}$ octahedra are formed, like in $SrRuO_4$ [16]. For $n=2$ double layers of fused $[TiO_6]^{8-}$ octahedra occur, for example in $Sr_3Ti_2O_7$ [17]. For $n=3$ there are examples such as $K_2Nd_2Ti_3O_{10}$ and $Ca_4Ti_3O_{10}$, which show triple blocks of $^2_\infty\{[TiO^{v}_{4/2}O^{t}_{2/1}]^{4-}\}$ layers of vertex-connected octahedra [18, 19]. In the Ruddlesden-Popper phases for $n>1$ the A^{n+} cations can have coordination numbers 9 or 12. The rare-earth elements prefer mostly the 12-fold coordination and alkali metals settle with the ninefold coordination, for example in $K_2SrTa_2O_7$ [20].

Ruddlesden-Popper phases $A_{n+1}B_nO_{3n+1}$ with $n=1$, 2, and 3 are of particular relevance, because they often exhibit interesting properties, such as ionic conductivity [21], phase transitions [22], and magnetic ordering [23], and because they can be exfoliated [24]. The substitution of an A^{2+} cation (A = alkaline-earth element) with

***Corresponding author: Thomas Schleid,** Institut für Anorganische Chemie, Universität Stuttgart, Pfaffenwaldring 55, D-70569 Stuttgart, Germany, e-mail: schleid@iac.uni-stuttgart.de
Christian Funk: Institut für Anorganische Chemie, Universität Stuttgart, Pfaffenwaldring 55, D-70569 Stuttgart, Germany; and Versuchsanstalt für Stahl, Holz und Steine, Karlsruher Institut für Technologie, Otto-Ammann-Platz 7, D-76131 Karlsruhe, Germany
Jürgen Köhler: Max-Planck-Institut für Festkörperforschung, Heisenbergstraße 1, D-70569 Stuttgart, Germany

two A'^{+} cations (A' = alkali element) in this structure type results in a series of compounds with the general formula $A'A_{n-1}M_nO_{3n+1}$ [25]. Substitution with small Li^+ cations leads to distorted $[LiO_4]^{7-}$ tetrahedra connecting the layers of octahedral polyhedra, as e.g. in $Li_2SrTa_2O_7$ [23, 26]. Replacing Sr^{2+} with Eu^{2+} cations in this structure type results in the magnetically interesting system $Li_2Sr_{1-x}Eu_xTa_2O_7$ ($0.8 > x > 1.0$) [23]. Besides other compositions derived from these series [27], Bhuvanesh et al. also obtained layered defect perovskites like $Li_4Sr_3Nb_6O_{20}$ [28]. We have prepared a series of such phases with lithium in fourfold (tetrahedral) and europium (sometimes along with K^+) in 12-fold (cuboctahedral) coordination, on which we report here.

2 Experimental

2.1 Sample preparation

2.1.1 Synthesis of $Li_2Eu_2Nb_3O_{10}$ and $Li_2Eu_{1.5}Ta_3O_{10}$

The syntheses of $Li_2Eu_2Nb_3O_{10}$ and $Li_2Eu_{1.5}Ta_3O_{10}$ were performed by heating mixtures from stoichiometric quantities of $Li_2[CO_3]$ (Acros Organics, Geel), Eu_2O_3 (ChemPur, 99.99%), Nb_2O_5 (Fluka, 99.9%) and Ta_2O_5 (ChemPur, 99.99%), respectively, and niobium (CIBA, reinst) and tantalum (Merck, 99.999%) metal powder, respectively, as described in the following equations:

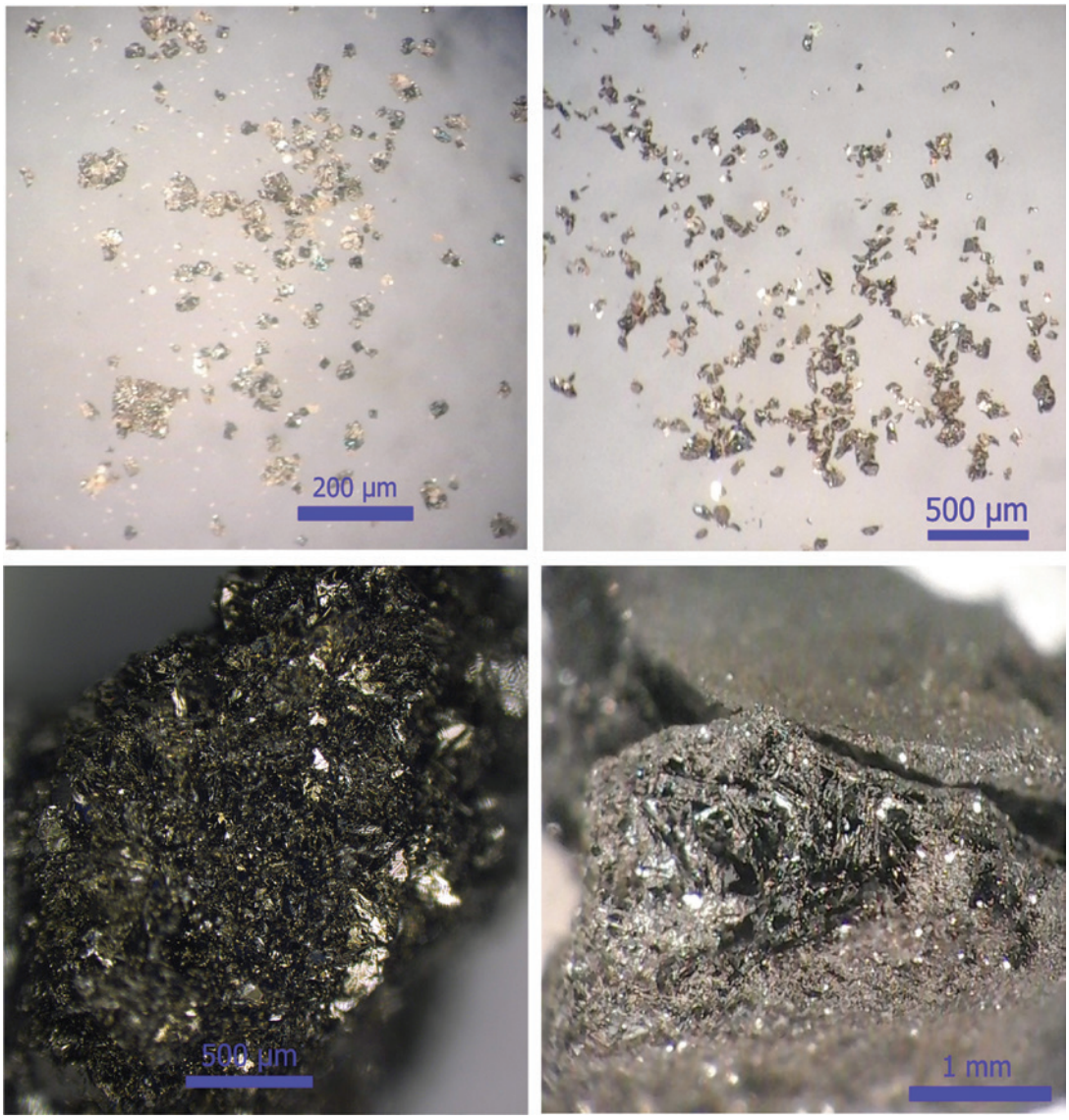

Fig. 1: Samples of $Li_2EuKNb_3O_{10}$ (top left), $Li_2Eu_2Nb_3O_{10}$ (top right), $Li_2Eu_{1.5}Ta_3O_{10}$ (bottom left), and $Li_2EuKTa_3O_{10}$ (bottom right) under a light microscope.

$$5\,Li_2[CO_3] + 5\,Eu_2O_3 + 6\,Nb_2O_5 + 3\,Nb \rightarrow 5\,Li_2Eu_2Nb_3O_{10} + 5\,CO_2\uparrow$$

$$20\,Li_2[CO_3] + 15\,Eu_2O_3 + 27\,Ta_2O_5 + 6\,Ta \rightarrow 20\,Li_2Eu_{1.5}Ta_3O_{10} + 20\,CO_2\uparrow$$

These reactions were performed in cramped, but not soldered niobium or tantalum capsules (Plansee, Reutte), which were heated in a high-frequency furnace above $T = 1600$°C for 10 min under an argon atmosphere. The melting cakes were cooled to room temperature within 10 min and black, crystalline products (Fig. 1) were obtained. The crystals remain unchanged in air for months.

2.1.2 Synthesis of $Li_2EuKNb_3O_{10}$ and $Li_2EuKTa_3O_{10}$

The syntheses of $Li_2EuKNb_3O_{10}$ and $Li_2EuKTa_3O_{10}$ were performed by heating mixtures from stoichiometric quantities of $Li_2[CO_3]$, $K_2[CO_3]$ (Merck, 99.0%), Eu_2O_3, Nb_2O_5 or Ta_2O_5 and niobium or tantalum metal powder (M = Nb or Ta), respectively, according to

$$10\,Li_2[CO_3] + 5\,Eu_2O_3 + 5\,K_2[CO_3] + 14\,M_2O_5 + 2\,M \rightarrow 10\,Li_2EuKM_3O_{10} + 15\,CO_2\uparrow$$

These mixtures were heated for 10 min as described above and cooled to room temperature within 10 more min. Black compact products were obtained and removed mechanically from the metal containers (Fig. 1). Both compounds are stable in air for several months.

2.2 Structure determinations

For the single-crystal X-ray diffraction studies, well-faceted crystals were selected under a light microscope, packed in 0.1 mm diameter glass capillaries and sealed. The crystals were measured at room temperature on a κ-CCD diffractometer (Bruker-Nonius) with Mo$K\alpha$ radiation ($\lambda = 71.07$ pm). The crystallographic data for $Li_2EuKNb_3O_{10}$, $Li_2Eu_2Nb_3O_{10}$, $Li_2Eu_{1.5}Ta_3O_{10}$, and $Li_2EuKTa_3O_{10}$ and the results of the final refinements are listed in Table 1, the atomic coordinates appear in Table 2.

Further details of the crystal structure investigations may be obtained from Fachinformationszentrum Karlsruhe, 76344 Eggenstein-Leopoldshafen, Germany (fax: (+49) 7247-808-666, http://www.fiz-karlsruhe.de/request_for_deposited _data.html, E-Mail: crys-data@fiz-karlsruhe.de), on quoting the depository numbers CSD-1949876 to CSD-1949879.

Table 1: Crystallographic data of $Li_2Eu_2Nb_3O_{10}$, $Li_2Eu_{1.5}Ta_3O_{10}$, $Li_2EuKNb_3O_{10}$, and $Li_2EuKTa_3O_{10}$.

	$Li_2Eu_2Nb_3O_{10}$	$Li_2Eu_{1.5}Ta_3O_{10}$	$Li_2EuKNb_3O_{10}$	$Li_2EuKTa_3O_{10}$
Crystal system	tetragonal			
Space group	*I*4/*mmm* (no. 139)			
Formula units per unit cell	$Z = 2$			
a/pm	393.47(2)	394.29(2)	395.64(2)	395.12(2)
c/pm	2687.91(18)	2609.42(16)	2635.28(17)	2612.53(15)
c/a	6.831	6.618	6.661	6.612
D_x/g · cm^{-1}	5.86	7.67	5.68	7.58
M/g · mol^{-1}	1361.10	1889.34	1287.34	1815.58
Diffractometer	κ-CCD (Bruker-Nonius)			
Radiation; λ/pm	Mo$K\alpha$; 71.07			
Temperature; T/K	293			
$h = k$, l	±5, ±34	±5, ±34	±5, ±34	±5, ±33
$2\theta_{max}$/°	54.94	55.16	54.92	54.73
F(000)/e	607	799	582	774
μ/mm^{-1}	17.8	51.4	15.9	49.7
Measured reflections	5243	3640	3005	4502
Independent reflections	189	187	188	185
R_{int}; R_σ	0.063; 0.018	0.091; 0.030	0.057; 0.021	0.063; 0.017
R_1; wR_2	0.022; 0.054	0.026; 0.067	0.022; 0.044	0.020; 0.051
GooF	1.073	1.170	1.159	1.124
$\rho_{max;\,min}$/e · Å^{-3}	1.29; −0.90	1.47; −1.76	1.02; −0.71	2.34; −1.47
CSD number	1949876	1949877	1949878	1949879

Table 2: Fractional atomic coordinates, site occupation factors (s.o.f.) and equivalent isotropic displacement parameters[a] (U_{eq}) for $Li_2Eu_2Nb_3O_{10}$, $Li_2Eu_{1.5}Ta_3O_{10}$, $Li_2EuKNb_3O_{10}$, and $Li_2EuKTa_3O_{10}$.

Atom	Wyckoff site	s.o.f.	*x*/*a*	*y*/*b*	*z*/*c*	U_{eq} /pm²	Atom	Wyckoff site	s.o.f.	*x*/*a*	*y*/*b*	*z*/*c*	U_{eq} /pm²
$Li_2Eu_2Nb_3O_{10}$							**$Li_2Eu_{1.5}Ta_3O_{10}$**						
Li	4*d*	1	0	1/2	1/4	411(67)	Li	4*d*	1	0	1/2	1/4	239(65)
Eu	4*e*	0.932(5)	0	0	0.42045(2)	149(3)	Eu	4*e*	0.725(6)	0	0	0.42092(4)	203(6)
Nb1	2*a*	1	0	0	0	101(5)	Ta1	2*a*	1	0	0	0	179(4)
Nb2	4*e*	1	0	0	0.15660(4)	112(4)	Ta2	4*e*	1	0	0	0.15629(2)	164(4)
O1	4*c*	1	0	1/2	0	510(62)	O1	4*c*	1	0	1/2	0	387(4)
O2	4*e*	1	0	0	0.0727(3)	183(23)	O2	4*e*	1	0	0	0.0740(4)	249(4)
O3	4*e*	1	0	0	0.2235(3)	169(21)	O3	4*e*	1	0	0	0.2278(4)	228(3)
O4	8*g*	1	0	1/2	0.1456(2)	160(14)	O4	8*g*	1	0	1/2	0.1484(3)	232(2)
$Li_2EuKNb_3O_{10}$							**$Li_2EuKTa_3O_{10}$**						
Li	4*d*	1	0	1/2	1/4	365(61)	Li	4*d*	1	0	1/2	1/4	263(73)
Eu	4*e*	0.782(5)	0	0	0.41985(3)	117(3)	Eu	4*e*	0.607(7)	0	0	0.42086(4)	129(5)
K	4*e*	0.218(5)	0	0	0.41985(3)	117(3)	K	4*e*	0.393(7)	0	0	0.42086(4)	129(5)
Nb1	2*a*	1	0	0	0	81(4)	Ta1	2*a*	1	0	0	0	114(3)
Nb2	4*e*	1	0	0	0.15761(4)	95(4)	Ta2	4*e*	1	0	0	0.15640(2)	111(3)
O1	4*c*	1	0	1/2	0	455(32)	O1	4*c*	1	0	1/2	0	346(41)
O2	4*e*	1	0	0	0.0742(3)	218(23)	O2	4*e*	1	0	0	0.0749(4)	164(30)
O3	4*e*	1	0	0	0.2272(3)	197(20)	O3	4*e*	1	0	0	0.2275(4)	101(23)
O4	8*g*	1	0	1/2	0.1492(2)	144(13)	O4	8*g*	1	0	1/2	0.1491(3)	157(18)

[a] $U_{eq} = 1/3(U_{11} + U_{22} + U_{33})$ [29].

3 Discussion

3.1 Crystal structures

$Li_2Eu_2Nb_3O_{10}$, $Li_2Eu_{1.5}Ta_3O_{10}$, $Li_2EuKNb_3O_{10}$, and $Li_2EuKTa_3O_{10}$ crystallize in the tetragonal space group *I*4/*mmm* typically found for Ruddlesden-Popper phases with lattice parameters ranging from $a = 393$ to 396 pm and from $c = 2609$ to 2688 pm (Fig. 2). The crystallographically independent Eu^{2+} cations are located in cuboctahedra formed by oxygen atoms. In all four compounds the Eu–O distances lie between 270 and 290 pm (Table 3), which is typical for europium atoms in the oxidation state +2 in agreement with the calculated bond-valence parameters (Table 4). These bond-valence parameters correspond well with the results from calculations of the Charge Distribution calculated with CHARDI2015 and the Madelung Parts of the Lattice Energy (MAPLE) [30–34]. It is remarkable that in $Li_2Eu_2Nb_3O_{10}$ the position of the europium atoms is fully occupied, in contrast to $Li_2Eu_{1.5}Ta_3O_{10}$, where only 3/4 of this position is filled with europium (Table 2). Simple charge counting thus results in the oxidation state +5 for tantalum in $Li_2Eu_{1.5}Ta_3O_{10}$, whereas an average oxidation state of +4.667 is obtained for niobium in $Li_2Eu_2Nb_3O_{10}$. For $Li_2EuKNb_3O_{10}$ and $Li_2EuKTa_3O_{10}$ a full occupation of the corresponding crystallographic sites with europium and potassium is found (Table 2). This appears reasonable, because of the comparable ionic radii of Eu^{2+} ($r_i = 148$ pm) and K^+ ($r_i = 164$ pm) for a 12-fold coordination [35, 36].

Taking the refined occupation factors of the crystallographic sites for europium and potassium in $Li_2EuKNb_3O_{10}$ and $Li_2EuKTa_3O_{10}$ into account, an oxidation of +5 results for both octahedrally coordinated atoms, niobium and tantalum, respectively. The polyhedra are vertex-connected forming $^2_\infty\{[MO^v_{4/2}O^t_{2/1}]^{3-}\}$ layers in the *ab* plane. Along the *c* direction, these layers form triple blocks (Fig. 2, top), which are separated by $^2_\infty\{[LiO^e_{4/2}]^-\}$ layers (Fig. 2, bottom), where the Li^+ cations are tetrahedrally coordinated (Fig. 3), but exhibit two extra oxygen contacts along [001].

3.2 Physical properties

The individual magnetic susceptibilities of $Li_2Eu_2Nb_3O_{10}$, $Li_2Eu_{1.5}Ta_3O_{10}$, and $Li_2EuKNb_3O_{10}$ were measured between $T = 5$ and 300 K in a SQUID magnetometer MPMS3 from

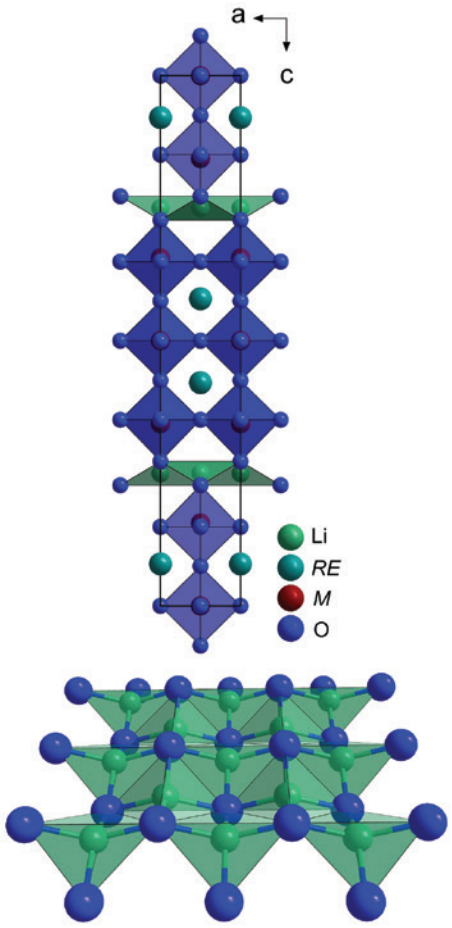

Fig. 2: Structural building units in $Li_2Eu_2Nb_3O_{10}$, $Li_2Eu_{1.5}Ta_3O_{10}$, $Li_2EuKNb_3O_{10}$, and $Li_2EuKTa_3O_{10}$ as extended unit cell viewed in *b* direction (top; *RE* = Eu or Eu and K, *M* = Nb and Ta) and a $^2_\infty\{[LiO^e_{4/2}]^-\}$ layer of edge-sharing $[LiO_4]^{7-}$ tetrahedra (bottom).

Quantum Design (San Diego) (Fig. 4). The susceptibilities follow a paramagnetic behavior in the measured temperature range (Table 5). Applying the Curie-Weiss law, the magnetic moments (μ_{eff}) were calculated to 6.31 μ_B ($Li_2Eu_2Nb_3O_{10}$), 7.89 μ_B ($Li_2Eu_{1.5}Ta_3O_{10}$), and 8.01 μ_B ($Li_2EuKTa_3O_{10}$). The theoretical moment for Eu^{2+} cations is 7.94 μ_B, so for $Li_2Eu_{1.5}Ta_3O_{10}$ and $Li_2EuKTa_3O_{10}$ it fits well, but for $Li_2Eu_2Nb_3O_{10}$ the moment is too small. As it is expected from the nearly full occupation of the europium site, niobium has to be partly reduced from +5 to +4. According to the findings from X-ray photo emission spectroscopy (XPS) studies, there are Nb^{4+} cations in the structure, which show van Vleck paramagnetism for a $4d^1$ configuration, leading to a calculated moment of 6.47 μ_B:

$$\mu_{theo} = \sqrt{\frac{3.72}{5.72}(\mu_{eff,Eu^{2+}})^2 + \frac{2}{5.72}(\mu_{eff,Nb^{4+}})^2}$$
$$= \sqrt{\frac{3.72}{5.72}(7.94\,\mu_B)^2 + \frac{2}{5.72}(1.73\,\mu_B)^2} = 6.47\,\mu_B$$

Table 3: Selected interatomic distances (*d*/pm) in the crystal structures of $Li_2Eu_2Nb_3O_{10}$, $Li_2Eu_{1.5}Ta_3O_{10}$, $Li_2EuKNb_3O_{10}$, and $Li_2EuKTa_3O_{10}$.

$Li_2Eu_2Nb_3O_{10}$							
Li	–O3	4×	209.1(4)	Nb1	–O2	2×	195.6(9)
	···Li	4×	278.1(1)		–O1	4×	196.6(1)
	···O4	2×	280.7(8)	Nb2	–O3	1×	180.0(1)
Eu	–O4	4×	265.3(5)		–O4	4×	198.8(1)
	–O2	4×	278.7(1)		–O2	1×	226.0(9)
	–O1	4×	290.7(1)				
$Li_2Eu_{1.5}Ta_3O_{10}$							
Li	–O3	4×	205.5(4)	Ta1	–O2	2×	192.9(9)
	···Li	4×	264.9(1)		–O1	4×	197.1(1)
	···O4	2×	278.8(8)	Ta2	–O3	1×	186.5(1)
Eu	–O4	4×	267.7(6)		–O4	4×	198.2(1)
	–O2	4×	279.1(1)		–O2	1×	215.0(9)
	–O1	4×	285.4(1)				
$Li_2EuKNb_3O_{10}$							
Li	–O3	4×	206.6(3)	Nb1	–O2	2×	195.7(8)
	···Li	4×	265.7(8)		–O1	4×	197.8(1)
	···O4	2×	268.7(5)	Nb2	–O3	1×	184.0(1)
Eu, K	–O4	4×	268.7(5)		–O4	4×	199.1(1)
	–O2	4×	280.2(1)		–O2	1×	219.6(8)
	–O1	4×	289.4(1)				
$Li_2EuKTa_3O_{10}$							
Li	–O3	4×	206.1(3)	Ta1	–O2	2×	195.6(9)
	···Li	4×	263.5(8)		–O1	4×	197.6(1)
	···O4	2×	279.4(1)	Ta2	–O3	1×	185.7(9)
Eu, K	–O4	4×	269.2(5)		–O4	4×	198.5(1)
	–O2	4×	279.6(1)		–O2	1×	213.0(9)
	–O1	4×	286.0(1)				

Table 4: Bond-valence sums [37] (calculated theoretical oxidation states) of the heavy-metal atoms in $Li_2Eu_2Nb_3O_{10}$, $Li_2Eu_{1.5}Ta_3O_{10}$, $Li_2EuKNb_3O_{10}$, and $Li_2EuKTa_3O_{10}$. The values given in *italics* have been calculated with the bond-valence parameter of Eu^{2+}.[a]

Wyckoff site	$Li_2Eu_2Nb_3O_{10}$	$Li_2Eu_{1.5}Ta_3O_{10}$	$Li_2EuKNb_3O_{10}$	$Li_2EuKTa_3O_{10}$
Eu in 4*e*	1.85; *2.24*	1.86; *2.25*	1.77; *2.14*	1.81; *2.19*
*M*1 in 2*a*	5.21	5.44	5.10	5.25
*M*2 in 4*e*	4.98	5.08	4.90	5.11

[a] $r_0(Eu^{2+} - O) = 2.147$ Å, $r_0(Eu^{3+} - O) = 2.076$ Å, $r_0(Ta^{5+} - O) = 1.920$ Å, $r_0(Nb^{5+} - O) = 1.911$ Å [29, 38, 39].

The cation-defect variant $Li_2Eu_{1.86(2)}\square_{0.14(2)}Nb_3O_{10}$ has been characterized by a single-crystal structure determination based on X-ray diffraction (Section 3.1). Such a deficiency at the europium site must be accompanied by the presence of niobium atoms which have an average oxidation state lower than +5. For an additional analysis of this oxoniobate, XPS spectra have been measured on a commercial Kratos Axis Ultra DLD system (Shimadzu,

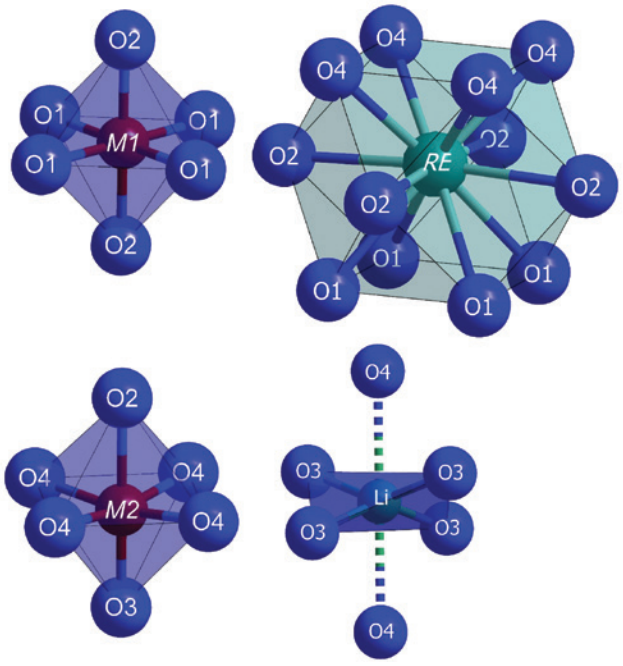

Fig. 3: Coordination polyhedra in $Li_2Eu_2Nb_3O_{10}$, $Li_2Eu_{1.5}Ta_3O_{10}$, $Li_2EuKNb_3O_{10}$, and $Li_2EuKTa_3O_{10}$ of *M*1 (top left) and *M*2 (bottom left, *M* = Nb or Ta) as octahedra, the cuboctahedral coordination sphere of the europium (or potassium) site (= *RE*, top right) and the lithium-centered oxygen tetrahedron (bottom right) with two extra oxygen neighbors along [001].

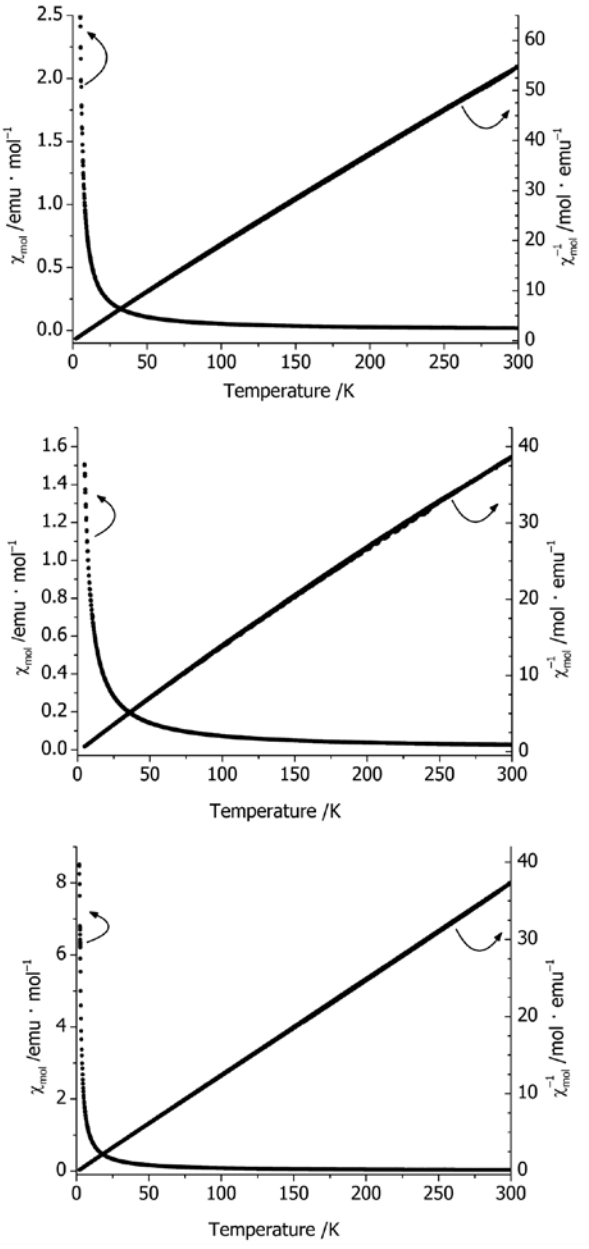

Fig. 4: Magnetic susceptibilities (χ_{mol}) and their inverse values (χ^{-1}_{mol}) as a function of temperature (T) for $Li_2Eu_{1.86(2)}\square_{0.14(2)}Nb_3O_{10}$ (top), $Li_2Eu_{1.5}Ta_3O_{10}$ (mid), and $Li_2EuKTa_3O_{10}$ (bottom).

Kyoto) with a monochromatized Al$K\alpha$ source (1486.6 eV) with a base pressure in the lower 10^{-10} mbar range. The binding energy (BE) was calibrated by setting the C 1s BE to 284.8 eV with respect to the Fermi level. High-resolution spectra were acquired with an analyzer pass energy of 20 eV. Analysis of the XPS data was performed with CasaXPS software. The measured polycrystalline samples were pressed into an indium foil. In their XPS spectra (Fig. 5) only europium atoms with the oxidation state +2 are observed and just minor impurities of Eu^{3+} can be detected, which probably stem from partial oxidation on the surface. However, as expected, besides Nb^{5+} a significant amount of Nb^{4+} is found, confirming the results from the structure refinement. The peak around 1200 eV in Fig. 5 (top) originates from small impurities of carbon arising from transportation processes of CO_2 during the high-temperature syntheses.

4 Conclusion

The new multinary oxides $Li_2Eu_2Nb_3O_{10}$, $Li_2Eu_{1.5}Ta_3O_{10}$, $Li_2EuKNb_3O_{10}$, and $Li_2EuKTa_3O_{10}$ with triple layers of

Table 5: Measured (μ_{eff}) and theoretical (μ_{theo}) magnetic moments as well as the applied magnetic fields (*H*) and the Weiss constants (θ) of $Li_2Eu_2Nb_3O_{10}$, $Li_2Eu_{1.5}Ta_3O_{10}$, and $Li_2EuKTa_3O_{10}$.[a]

Compound	μ_{eff}/μ_B	μ_{theo}/μ_B	θ (K)	*H*/Oe
$Li_2Eu_2Nb_3O_{10}$	6.31	6.47	−0.8(1)	500
$Li_2Eu_{1.5}Ta_3O_{10}$	7.89	7.94	−5.9(1)	500
$Li_2EuKTa_3O_{10}$	8.01	7.94	0.8(1)	250

[a]1 Oe = 7.96×10^3 A m^{-1}.

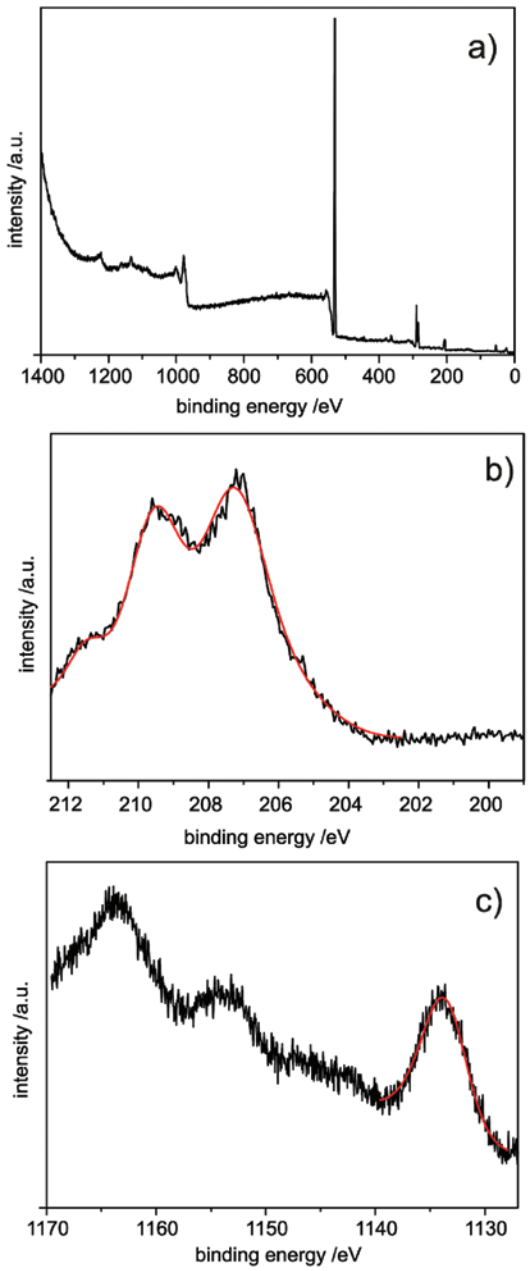

Fig. 5: a) XPS spectrum of $Li_2Eu_2Nb_3O_{10}$ in the range from $E = 0$ to 1400 eV, b) XPS spectrum of $Li_2Eu_2Nb_3O_{10}$ together with a simulation (red) in the range between 200 and 213 eV for the niobium transitions, c) transitions for europium together with simulations (red) in the range from 1127 to 1170 eV.

corner-sharing $[MO_6]^{7-}$ octahedra (M = Nb and Ta) including layers of edge-sharing $[LiO_4]^{7-}$ tetrahedra, have been synthesized for the first time using high-temperature solid-state reactions. They crystallize in the space group $I4/mmm$, typically found for Ruddlesden-Popper phases. A full occupation of the cation sites in $Li_2Eu_2Nb_3O_{10}$ leads to a mixed-valent oxoniobate(IV,V), whereas the structure of $Li_2Eu_{1.5}Ta_3O_{10}$ demonstrates the possibility of complex cationic non-stoichiometry that allows for the formation of an oxotantalate(V). Exfoliation of these compounds might lead to new low-dimensional magnetic materials with octahedral triple layers as found for the double-layer example $Li_2EuNb_2O_7$.

Acknowledgements: The authors thank Kathrin Küster (Max-Planck-Institut für Festkörperforschung, Stuttgart) for the measurements of the XPS spectra, Dr. Björn Blaschkowski (Institut für Anorganische Chemie, Universität Stuttgart) for the magnetic measurements and Dr. Falk Lissner (Institut für Anorganische Chemie, Universität Stuttgart) for the collection of the single-crystal X-ray diffraction data.

References

[1] A. R. von Hippel, *Rev. Mod. Phys.* **1950**, *22*, 221.
[2] G. J. McCarthy, J. E. Greedan, *Inorg. Chem.* **1975**, *14*, 772.
[3] Y. Zong, K. Fujita, H. Akamatsu, S. Murai, K. Tanaka, *J. Solid State Chem.* **2010**, *183*, 168.
[4] H. Akamatsu, K. Fujita, H. Hayashi, T. Kawamoto, Y. Kumagai, Y. Zong, K. Iwata, F. Oba, I. Tanaka, K. Tanaka, *Inorg. Chem.* **2012**, *51*, 4560.
[5] V. G. Zubkov, A. P. Tyutyunnik, V. A. Pereliaev, G. P. Shveikin, J. Köhler, R. K. Kremer, A. Simon, G. Svensson, *J. Alloys Compd.* **1995**, *226*, 24.
[6] A. Bussmann-Holder, J. Köhler, K. Roleder, Z. Guguchia, H. Keller, *Thin Solid Films* **2017**, *643*, 3.
[7] Y. Misawa, Y. Doi, Y. Hinatsu, *J. Solid State Chem.* **2011**, *184*, 1478.
[8] J. Brous, I. Fankuchen, E. Banks, *Acta Crystallogr.* **1953**, *6*, 67.
[9] T. Katsufuji, H. Takagi, *Phys. Rev. B* **2001**, *64*, 054415.
[10] P. Reuvekamp, R. K. Kremer, J. Köhler, A. Bussmann-Holder, *Phys. Rev. B* **2014**, *90*, 094420.
[11] P. Reuvekamp, K. Caslin, Z. Guguchia, H. Keller, R. K. Kremer, A. Simon, J. Köhler, A. Bussmann-Holder, *J. Phys.: Cond. Mat.* **2015**, *17*, 262201.
[12] Z. Guguchia, H. Keller, A. Bussmann-Holder, J. Köhler, R. K. Kremer, *Eur. Phys. J.* **2013**, *B 86*, 409.
[13] Ch. Funk, E. Brücher, J. Köhler, Th. Schleid, *Z. Kristallogr.* **2019**, *Suppl. 39*, 98.
[14] D. Montasserasadi, M. W. Granier, L. Spinu, S. C. Rai, W. Zhou, J. B. Wiley, *Dalton Trans*. **2015**, *44*, 10654.
[15] S. N. Ruddlesden, P. Popper, *Acta Crystallogr.* **1957**, *10*, 538.
[16] B. V. Beznosikov, K. S. Aleksandrov, *Crystallogr. Rep.* **2000**, *45*, 792.
[17] M. M. Elcombe, E. H. Kisi, K. D. Hawkins, T. J. White, P. Goodman, S. Matheson, *Acta Crystallogr.* **1991**, *B47*, 305.
[18] G. Amow, J. E. Greedan, *Acta Crystallogr*. **1998**, *C 54*, 1053.
[19] K. D. Hawkins, T. J. White, *Phil. Trans. Roy. Soc. London A* **1991**, *336*, 541.
[20] M. P. Crosnier-Lopez, F. Le Berre, J. L. Fourquet, *J. Mater. Chem.* **2001**, *11*, 1146.

[21] K. Toda, S. Kurita, M. Sato, *Solid State Ionics* **1995**, *81*, 267.
[22] T. Pagnier, N. Rosman, C. Galven, E. Suard, J. L. Forquet, F. Le Berre, M. P. Crosnier-Lopez, *J. Solid State Chem.* **2009**, *182*, 317.
[23] P. D. Battle, J. C. Burley, D. J. Gallon, C. P. Grey, J. Sloan, *J. Solid State Chem.* **2004**, *177*, 119.
[24] J. A. Schottenfeld, Y. Kobayashi, J. Wang, D. Macdonald, Th. E. Mallouk, *Chem. Mater*. **2008**, *20*, 213.
[25] B. V. Beznosikov, K. S. Aleksandrov, *Kristallografiya* **2000**, *45*, 864.
[26] N. Floros, C. Michel, M. Hervieu, B. Raveau, *J. Mater. Chem.* **1999**, *9*, 3101.
[27] Ch. Funk, J. Köhler, Th. Schleid, *Z. Kristallogr.* **2016**, *Suppl. 36*, 82.
[28] N. S. P. Bhuvanesh, M. P. Crosnier-Lopez, O. Bohnke, J. Emery, J. L. Fourquet, *Chem. Mater.* **1999**, *11*, 634.
[29] R. X. Fischer, E. Tillmanns, *Acta Crystallogr.* **1988**, *C44*, 775.
[30] M. Nespolo, B. Guillot, *J. Appl. Crystallogr.* **2016**, *49*, 317.
[31] R. Hoppe, *Angew. Chem. Int. Ed. Engl.* **1966**, *5*, 95.
[32] R. Hoppe, *Angew. Chem. Int. Ed. Engl.* **1980**, *19*, 110.
[33] R. Hoppe, *Z. Naturforsch.* **1995**, *50a*, 555.
[34] M. Nespolo, G. Ferraris, G. Ivaldi, R. Hoppe, *Acta Crystallogr.* **2001**, *B57*, 652.
[35] M. Allieta, M. Scavini, L. J. Spalek, V. Scagnoli, H. C. Walker, Ch. Panagopoulos, S. S. Saxena, T. Katsufuji, C. Mazzoli, *Phys. Rev. B* **2012** *85*, 184107-1–8.
[36] R. D. Shannon, *Acta Crystallogr.* **1976**, *A32*, 751.
[37] I. D. Brown, D. Altermatt, *Acta Crystallogr.* **1985**, *B41*, 244.
[38] N. E. Brese, M. O'Keeffe, *Acta Crystallogr.* **1991**, *B47*, 192.
[39] F. Zocchi, *J. Mol. Struct. THEOCHEM* **2007**, *805*, 73.